Direct imaging of commensurate vortex structures in ordered antidot arrays

A. N. Grigorenko, G. D. Howells, and S. J. Bending*
Department of Physics, University of Bath, Claverton Down, Bath BA2 7AY, United Kingdom

J. Bekaert, M. J. Van Bael, L. Van Look, V. V. Moshchalkov, and Y. Bruynseraede
Laboratorium voor Vaste-Stoffysica en Magnetisme, Katholieke Universiteit Leuven, Celestijnenlaan 200D, 3001 Leuven, Belgium

G. Borghs
IMEC, Kapeldreef 75, 3001 Leuven, Belgium

I. I. Kaya
The Rowland Institute for Science, 100 Edwin H. Land Boulevard, Cambridge, Massachusetts 02142

R. A. Stradling
Imperial College of Science Technology and Medicine, Prince Consort Road, London SW7 2AZ, United Kingdom
(Received 19 June 2000; published 11 January 2001)

A high resolution scanning Hall probe microscope has been used to investigate flux line dynamics and pinning phenomena in a thin Pb film containing a square array of artificial pinning sites (antidots). We observe directly that a maximum of two flux quanta can be pinned at a single antidot at low temperatures (5.5 K), in reasonable agreement with theoretical predictions. Using the scanning Hall probe to measure the ''local magnetization'' as a function of applied field, as well as image flux line structures in the same sample, allows us to directly correlate the two data sets. Peaks in the local magnetization at rational fractional matching fields can generally be linked to ordered commensurate vortex structures that maximize the mean vortex spacing. We find the commensurate vortex structures to be very stable, but excess vortices or vacancies, formed when the applied field deviates slightly from integer filling, are mobile on the time scale of image acquisition. Data are also presented where a domain wall between two ordered commensurate domains could be clearly resolved.

DOI: 10.1103/PhysRevB.63.052504 PACS number(s): 74.60.Ge, 07.79.−v, 74.25.Ha, 74.76.Db

Recent advances in microfabrication technology have made it possible to produce superconducting thin films with carefully controlled arrays of artificial pinning centers, e.g., an ordered array of holes or ''antidots'' as considered here.[1–4] Such systems are of great interest in two respects. First, an antidot represents a model microscopic pinning site for single quantum or multiquanta vortices (carrying flux $n\phi_0$) and allows a direct comparison between experiment and theory; an area where existing understanding is incomplete. We have used a high resolution scanning Hall probe microscope (SHPM) to measure directly the maximum flux $n\phi_0$, which can be pinned at a single antidot at low temperatures and found reasonably good agreement with theoretical predictions.[5,6] Second, it is now well known that commensurate vortex structures at rational fractional filling of the antidot lattice lead to pronounced enhancements of the bulk magnetization (M) and critical current (j_c) of the superconductor.[1–4] Ordered flux line structures with various symmetries have been imaged using Lorentz microscopy,[7] but to date it has not been possible to make a more direct comparison between magnetic images and magnetization data. We have been able to measure ''local magnetization'' on the same regions of the sample where vortex images were generated, allowing the two data sets to be directly correlated. We observe peaks in the local magnetization at rational fractional matching fields that can generally be linked to ordered commensurate vortex structures at lower temperatures. We find these structures to be very stable, but excess vortices or vacancies formed when the applied field deviates slightly from integer filling are mobile on the time scale of image acquisition even when they are sited at antidots.

The sample investigated here consists of an 80-nm-thick Pb film ($T_c = 7.1$ K) containing a periodic square array (period $a = 1.5$ μm) of approximately circular holes with a diameter of 660 nm patterned by electron beam lithography and lift-off. Although bulk Pb is a type-I superconductor, it becomes type II in thin film form as a result of the reduced dimensionality as well as surface and grain boundary scattering. The superconducting film is covered with a protective 20-nm Ge layer and a 10-nm Au coating to facilitate scanning tunneling microscope (STM) control of the SHPM. Further details of the sample fabrication and characterization are given elsewhere.[8]

The SHPM used is a modified commercial low temperature STM in which the usual tunneling tip has been replaced by a microfabricated GaSb/InAs/GaSb chip. A Hall probe was defined in the InAs quantum well at the intersection of two ~300 nm-wide wires approximately 5 μm from the corner of a deep mesa etch. The latter had been coated with a thin Au layer to act as an integrated STM tip. The sample is first approached towards the sensor until tunneling is established and then retracted about 100 nm allowing rapid scanning. The Hall probe makes an angle of about 1° with the sample plane so that the STM tip is always the closest point to the surface and the Hall sensor was about 300–400 nm above the sample in the images shown here. In order to sup-

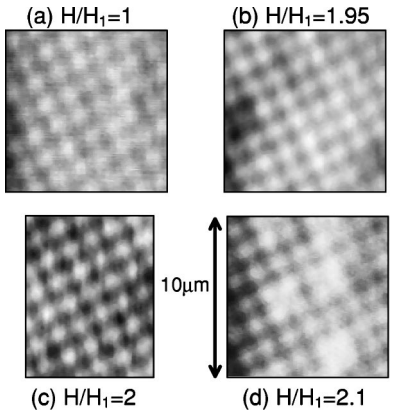

FIG. 1. SHPM scans after field-cooling to 5.5 K in (a) $H=H_1$, (b) $H=1.95H_1$, (c) $H=2H_1$, and (d) $H=2.1H_1$.

press random telegraph noise, which is always present in submicron Hall probes, the images presented here are the result of averaging 100 frames of the same region of the sample captured over a total period of about 15 min. A more detailed description of the instrument is given elsewhere.[9]

The interaction between a flux line in a bulk type-II superconductor and a hollow tube of radius R was calculated almost 30 years ago by Mkrtchyan and Schmidt.[5] They found that the first ϕ_0 vortex is always attracted to the empty hole while the interaction is always repulsive when at least a flux $n_s\phi_0$ (where n_s is called the saturation number) is trapped in the hole. Between these two limiting cases the interaction is repulsive at long ranges and attractive at short ranges, giving one insight into how complicated and history-dependent pinning phenomena in superconductors can be. In the limit that the Ginzburg-Landau parameter $\kappa \gg 1$ and $1/\kappa \ll R/\lambda \ll 1$, where λ is the magnetic field penetration depth, these authors found the following expression for the saturation number

$$n_s(T)=R^2/[\xi(T)^2+2\xi(T)R], \tag{1}$$

where $\xi(T)$ is the temperature-dependent coherence length of the superconductor. We note that our thin film geometry is different from the one used to derive this expression but, in the absence of other theoretical work, Eq. (1) provides a useful estimate of $n_s(T)$. The saturation number for ''blind'' holes of varying diameter in a superconducting film has been studied previously in a series of one-shot Bitter decoration experiments.[10] In contrast we are able to study trapped flux structures in the same sample as the applied field is smoothly increased. Measurements of the upper critical field of an unpatterned Pb film that was otherwise identical to that studied here yielded an estimate of the coherence length in the film plane of $\xi_{\parallel}(0)=30$ nm. Assuming that the antidots are round with a radius of 330 nm, and a dirty limit Ginzburg-Landau-type temperature dependence for $\xi_{\parallel}(T)$, we estimate the saturation number from Eq. (1) to be $n_s=1$ $(6 \leqslant T < T_c = 7.1$ K) and $n_s=2$ $(4.5 \leqslant T < 6$ K). Buzdin[6] calculated that the antidot occupancy $2\phi_0$ will also be *energetically* stable over the ϕ_0 occupancy if $R^3 < \xi(T)\lambda(T)^2$, a condition that is satisfied for $T < 0.99T_c$. Figure 1 shows a set of four high

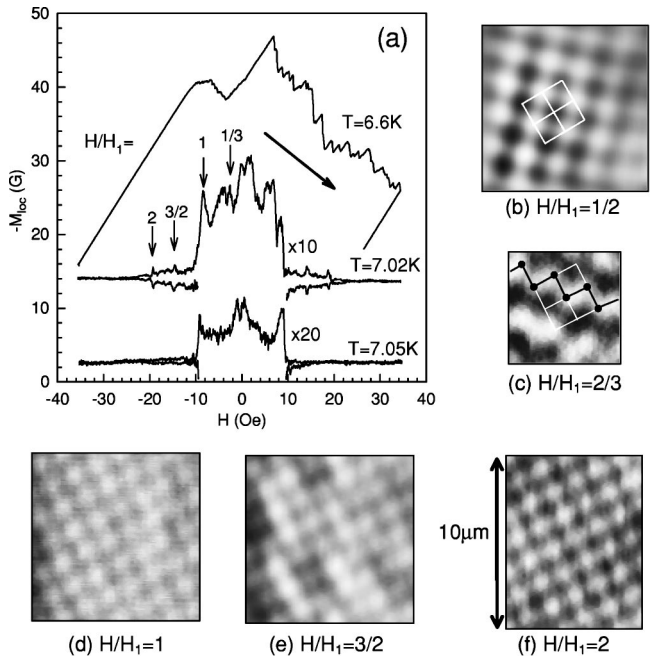

FIG. 2. (a) ''Local magnetization'' loops (offset for clarity) measured with a Hall probe above the antidot array at three different temperatures. SHPM scans after field-cooling to 5.5 K in (b) $H=H_1/2$ (white lines indicate the location of four unit cells of the antidot lattice), (c) $H=2H_1/3$ (black lines and symbols indicate the positions of one chain of flux lines, white lines outline four unit cells of the antidot lattice), (d) $H=H_1$, (e) $H=3H_1/2$, and (f) $H=2H_1$.

resolution SHPM images captured after field-cooling to 5.5 K in various magnetic fields applied perpendicular to the plane of the sample (expressed as fractions of the first matching field $H_1 \equiv \phi_0/a^2=9.2$ Oe). At the first matching field [Fig. 1(a)], we clearly resolve an ordered periodic flux structure with a ϕ_0 vortex (bright spot) trapped at each antidot. At exactly twice the matching field [Fig. 1(c)] we again observe an ordered vortex structure where there is now a flux $2\phi_0$ per antidot. A small defect (probably a dust particle on the surface) on the left of image 1(c) [and 2(f)] has been clipped off. If the field deviates slightly below $2H_1$ [e.g., Fig. 1(b), $H/H_1=1.95$] we observe on-site vacancies (i.e., ϕ_0 instead of $2\phi_0$ vortices) while slightly above it [e.g., Fig. 1(d), $H/H_1=2.1$] we find interstitial excess vortices. The latter have a characteristic square appearance as the tails of the interstitial flux lines overlap with the four on-site nearest neighbors making them also appear brighter. We conclude therefore, that for our system, $n_s=2$ at 5.5 K (as it is down to 5 K, the lowest operation temperature of our microscope). The saturation number always falls to unity close to T_c as the coherence length diverges, but we are unable to establish the exact crossover temperature for our system as the image contrast gets too poor to resolve vortices at higher temperatures. We note that our thin film geometry does not correspond to the bulk sample assumed in the derivation of Eq. (1) nor are we in the limit $R/\lambda \ll 1$ $[R/\lambda(5.5K) \sim 2]$. In this light, the semiquantitative agreement between the observed and calculated saturation numbers is surprisingly good.

In contrast to bulk samples where the repulsive vortex-vortex potential decays exponentially with separation, vortices in continuous thin films interact over long distances via the stray fields in the surrounding free space.[11] Evidence exists,[4] however, that the bulk penetration depth is indeed appropriate for perforated thin films of the type considered here. As $\lambda(T)$ diverges close to T_c, long-range interactions promote ordering phenomena in samples containing periodic antidot arrays, which can strongly influence magnetization curves provided the pinning in unpatterned ''reference'' films is not too strong. Figure 2(a) shows ''local magnetization'' ($\mu_0 M_{loc} = B_{loc} - \mu_0 H$) loops as a function of swept applied magnetic field (point resolution 0.07 Oe, time to obtain one loop ~ 5 mins) captured with a 0.8-μm resolution Hall probe at a fixed position a few microns above the sample surface. Close to T_c, pronounced peaks are observed in M_{loc} when a commensurate flux structure ''locks in'' beneath the Hall probe. Under these conditions there will be no change in local magnetic induction as the applied field is varied over a finite range, generating peaks when the local magnetization is constructed. A clear advantage of the Hall probe is that it is sensitive to the presence of small ordered domains, in contrast to bulk magnetization measurements,[2,3,12] where large terraces, occupying a major fraction of the sample are required. At 7.05 K, two peaks at $\pm H_1$ dominate the data, while the magnetization collapses almost to zero for $|H| > H_1$, indicating the presence of highly mobile excess vortices and the fact that the first matching field is only just below H_{c2} for the film. Since these excess vortices are most likely located at interstitial positions we presume that $n_s = 1$ at this temperature. We also observe a dense spectrum of fine structure in the range $H_1/10 < |H| < H_1$, which is well above the noise level of our detection system, indicating that a very large number of stable commensurate states can form very close to T_c when the penetration depth becomes large, random bulk pinning is weak, and extremely long-range correlations are possible. The dip in M_{loc} around $H = 0$ suggests that enhanced pinning due to ordering is ineffective at very low fields. At a slightly lower temperature of 7.02 K, a few rational filling fractions begin to dominate the data. We clearly observe peaks at $H_1/3$, H_1, $3H_1/2$, and $2H_1$ while less well-resolved (presumably due to the close proximity of other stable fractions) structure also exists close to $H_1/2$ and $2H_1/3$. There is a clear asymmetry in the height of the peaks in magnetization at $\pm H_1$ with respect to sweep direction with the strongest features visible when the magnetic field is ramped from high ($|H| > H_1$) to low ($|H| < H_1$). Since we presume that excess interstitial vortices (sweep down) have a higher mobility than on-site vacancies (sweep up), we attribute this to different ordering rates for these two types of objects. At low temperatures (e.g., 6.6 K), the fine structure in M_{loc} no longer correlates well with the filling factor. At these temperatures the magnetization is quite high, and large induction gradients inside the sample can be supported. As a consequence filling factors are different at different locations in the sample and matching effects are averaged over. In this case the data should be analyzed in terms of a critical state model.[13,14]

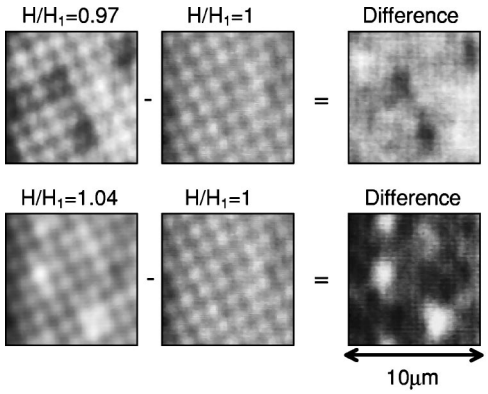

FIG. 3. SHPM scans and difference images after field-cooling to 5.5 K in a field slightly below and slightly above the first matching field.

The flux structures responsible for the observed enhancements in M and j_c are believed to correspond to ordered configurations where vortices try to maximize their mean separation subject to the imposed pinning array. Ordered structures of this type have been predicted by simulations[15] but have only been verified experimentally in a few cases[7] and even then only when $n_s = 1$. Unfortunately the field contrast is too weak near T_c for us to resolve discrete vortices and we have to cool the sample to 5.5 K in order to image the vortex configurations directly. Since the saturation number almost certainly increases upon cooling the link between the data sets becomes tenuous for $H > H_1$, but should be rigorous for $H \leqslant H_1$. Figures 2(b)–2(f) show a family of images captured after field cooling to 5.5 K at various applied magnetic fields. At $H_1/2$ [Fig. 2(b)] the well-known ''checkerboard'' structure is seen where every second pinning site is occupied on a square lattice rotated at 45° to the underlying pinning lattice. For $2H_1/3$ [Fig. 2(c)] we observe a striped flux phase with vortices lying in a zigzag pattern diagonally across the pinning array with an empty chain in between. This image is smaller than the rest due to the small size of ordered domains at this filling factor. Ordering at $H_1/3$ was also observed and was the complement of Fig. 2(c). At H_1 [Fig. 2(d)] and $2H_1$ [Fig. 2(f)], we see the ordered ϕ_0 and $2\phi_0$ states described earlier. At $3H_1/2$ [Fig. 2(e)], the image shows rather little order, although one might guess that it would reflect the superposition of $H_1/2$ and H_1. Indeed there appears to be a pronounced tendency for the formation of short chains of $2\phi_0$ vortices running from top left to bottom right in the image. We do not fully understand the origin of these structures but speculate that they may be formed as a result of the change in saturation number at temperatures somewhat below the critical temperature and note that more rapid ordering is to be expected close to T_c.

Although the imaged commensurate states presented in Fig. 2 are very stable on the time scale of image acquisition, the same is not true of structures formed when the filling deviates slightly from integer filling. This is illustrated in Fig. 3 where an image at $H = H_1$ has been subtracted from images slightly below and slightly above the first matching field (all field-cooled to 5.5 K). The applied field is calibrated with high precision, as is the expected difference in

the average number of flux lines in the two images. We calculate that the $(0.97H_1 - H_1)$ difference image should contain about one $(1.3\phi_0)$ down (black) vortex while we actually observe three rather irregular black objects. We speculate that a single vacancy has jumped between three different locations in the course of capturing the 100 scans that were averaged to generate this image. Both the amplitude of the features observed and the presence of weak white spots at the positions of the vacancies in the image at $0.97H_1$ confirm this conclusion. Likewise the $(1.04H_1 - H_1)$ difference image should contain about two $(1.8\phi_0)$ up (white) vortices while we see at least four very irregular white objects. One of these (lower right corner) appears to be a rare vortex at an interstitial site, whose amplitude indicates that it may not have moved, but the other weaker objects appear to arise from an on-site excess flux line hopping between different sites.

Finally we briefly discuss the extent of the ordered domains imaged here. Recently, Field *et al.*[16] showed a fascinating variety of possible domain structures in square pinning arrays at different fractional fillings. Due to the smaller scan area of our high resolution microscope it is more difficult for us to clearly establish the extent of domains. Figure 4, however, shows an image after field-cooling to 5.5 K at $H_1/2$ where a domain wall between the two degenerate checkerboard states is clearly resolved. The high-energy wall consists of a bond between flux lines, one lattice spacing apart, running diagonally across the image from bottom left to upper right. In this case we believe it is likely that the domain wall forms due to a very rare defect in the lithography just outside of the scanned region (probably one of the Pb dots failed to come out during lift-off). Whether there are more fundamental factors controlling the sizes of domains at different filling fractions is, however, a very interesting question which should be addressed in future experiments.

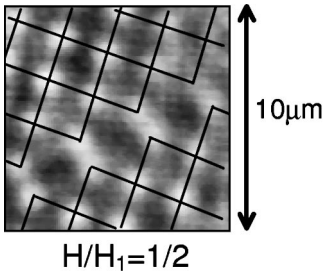

FIG. 4. SPHM scan after field-cooling to 5.5 K at $H = H_1/2$. The black lines indicate the two ordered pinned vortex domains separated by a domain wall running diagonally across the image.

In conclusion, scanning Hall-probe microscopy has been used to investigate flux structures in a Pb film containing a square antidot array. We find that a maximum of two flux quanta can be pinned at a single antidot at 5.5 K in reasonable agreement with theoretical predictions. We are able to correlate peaks in the ''local magnetization'' at rational fractional matching fields with the expected commensurate vortex structures for $0 \leqslant H \leqslant H_1$, but do not observe ordered vortex images for $H_1 < H < 2H_1$. The commensurate vortex structures appear to be very stable, but excess vortices or vacancies, formed when the applied field deviates slightly from integer filling, are mobile on the time scale of image acquisition.

This work was supported in the UK by EPSRC and MOD Grants Nos. GR/J03077 and GR/L96448 as well as the University of Bath Initiative Fund, by ESF Program VORTEX and in Belgium by the Fund for Scientific Research–Flanders (FWO), the Belgian IUAP, and the Flemish GOA programs.

*Electronic address: pyssb@bath.ac.uk

[1] A.T. Fiory, A.F. Hebard, and S. Somekh, Appl. Phys. Lett. **32**, 73 (1978).
[2] M. Baert *et al.*, Phys. Rev. Lett. **74**, 3269 (1995).
[3] M. Baert *et al.*, Europhys. Lett. **29**, 157 (1995).
[4] V.V. Moshchalkov *et al.*, Phys. Rev. B **57**, 3615 (1998).
[5] G.S. Mkrtchyan and V.V. Schmidt, Zh. Éksp. Teor. Fiz. **61**, 367 (1971) [Sov. Phys. JETP **34**, 195 (1972)].
[6] A.I. Buzdin, Phys. Rev. B **47**, 11 416 (1993).
[7] K. Harada *et al.*, Science **274**, 1167 (1996).
[8] Y. Bruynseraede *et al.*, Phys. Scr. **42**, 37 (1992).
[9] A. Oral, S.J. Bending, and M. Henini, Appl. Phys. Lett. **69**, 1324 (1996).
[10] A. Bezryadin and B. Pannetier, J. Low Temp. Phys. **102**, 73 (1996).
[11] J. Pearl, Appl. Phys. Lett. **5**, 65 (1964).
[12] V. Metlushko *et al.*, Phys. Rev. B **59**, 603 (1999); J.I. Martin *et al.*, Phys. Rev. Lett. **83**, 1022 (1999).
[13] L.D. Cooley and A.M. Grishin, Phys. Rev. Lett. **74**, 2788 (1995).
[14] V.V. Moshchalkov *et al.*, Phys. Rev. B **54**, 7385 (1996).
[15] C. Reichhardt, C.J. Olson, and F. Nori, Phys. Rev. B **57**, 7937 (1998).
[16] S.B. Field *et al.*, cond-mat/0003415 (unpublished).